Hindawi
Advances in Materials Science and Engineering
Volume 2023, Article ID 8622525, 7 pages
https://doi.org/10.1155/2023/8622525

Research Article

Experimental Studies on Mechanical Behavior of TIG and Friction Stir Welded AA5083 -AA7075 Dissimilar Aluminum Alloys

Veeraiah Goriparthi,[1,2] **Ramanaiah Nallu**,[2] **Rohinikumar Chebolu**,[2] **Sudhakar Indupuri**,[1] **and Ramesh Rudrapati**[3]

[1]*Department of Mechanical Engineering, Maharaj Vijayaram Gajapathi Raj College of Engineering, Vizianagaram 535005, India*
[2]*Department of Mechanical Engineering, A.U. College of Engineering, Andhra University, Visakhapatnam 530003, Andhra Pradesh, India*
[3]*Department of Mechanical Engineering, Bulehora University, Bule Hora, Ethiopia*

Correspondence should be addressed to Ramesh Rudrapati; rameshrudrapati@gmail.com

Received 28 November 2022; Revised 15 December 2022; Accepted 18 March 2023; Published 14 April 2023

Academic Editor: B. Radha Krishnan

Welding is a suitable and better process to manufacture complex objects for aerospace, naval, and automotive structures. Service conditions and complexity in load acting force the manufactures to make joints between dissimilar materials. Thus, there is a need for efficient welding techniques to form sound joints and an understanding of imperfections and their effects. In this study an attempt has been made to study the joining feasibility of dissimilar aluminum alloys by two different welding techniques, namely, tungsten inert gas welding (TIG) and friction stir welding (FSW). Dissimilar AA5083-O and AA7075-T651 aluminum alloys successfully joined by considered welding techniques. Metallurgical and mechanical characteristics of fabricated weld joints are studied at different weld currents (80–120 amp) for TIG and various rotational speeds (800, 1000, 1100, 1200, and 1400 rpm) with constant traverse speed for FSW. Weld joints made by FSW exhibit superior tensile strength, whereas the joint line microhardness of TIG samples is higher than the FSW ones.

1. Introduction

The need for light weight, low cost, high strength, and altered feature materials are the requirement of industries like aerospace, shipbuilding, and transportation. For instance, structures need high resistance against high temperature for some period of time and excellent resistance to corrosion at other times. Similarly, parts need high wear resistance at some areas and excellent strength at some locations. All these mentioned features are satisfied by aluminium alloys. However, due to incompatibility in material properties like physical, chemical, and mechanical, joining of dissimilar materials or aluminum alloys could be a difficult task. Also, because of variation in thermal expansion coefficient and solidus temperature, there is a chance to fail even during the welding process [1, 2]. Fusion-based and solid state welding techniques as well as other processes such as soldering and brazing can be successfully used to join aluminum alloys. Fusion-based techniques like gas tungsten arc welding (GTAW or TIG) and gas metal arc welding (GMAW or MIG), oxy-hydrogen welding, oxy-acetylene welding, air-acetylene welding, and plasma arc welding are used to join aluminum alloys. Among the mentioned techniques, GTAW is the most popular one to join aluminum alloys. However, poor selection of process parameters results in solidification shrinkage, intermetallic phases, formation of intergranular microcracks and stress corrosion cracking, and unpredictable failure of the joints during the service period [3, 4]. Solid state techniques like friction welding, brazing, soldering, explosion welding, ultrasonic welding, diffusion welding and friction stir welding can mitigate the problems that arise in fusion based processes [5]. In the present study two welding

techniques fusion-based (TIG) and solid state welding (FSW) are considered for joining of AA5083 and AA7075 dissimilar aluminum alloys.

GTWA (TIG) welding is fusion-based; an arc welding process developed in the year 1940 to join magnesium and aluminum alloys. GTAW uses a nonconsumable electrode, and an arc is developed between the electrode and the part to be welded. An insulating gas between the electrode and base material is broken down by a high voltage, and then the arc is developed due to the transfer of current through the electrode. The developed arc generates intense heat and joins the part with or without filler material. An inert gas like helium and argon is used to protect the electrode and molten weld pool from oxidation. The welding process parameters (current, welding speed, and shielding gas flow rate) influence the weld bead quality [6].

Friction stir welding (FSW), a novel technique patented by the welding institute, UK, in the year 1991 seems to be the alternative to conventional welding techniques due to the low cost, reduced weight, lower energy consumption, reduced greenhouse gasses, and better metallurgical properties [7]. FSW is an autogenous and continuous hot shearing process that occurs below solidus temperature of materials to be joined. A nonconsumable rotating tool harder than the materials to be joined plunges into the abutting edges of the plates to be joined and moves along the joint line during the welding process. The base material is placed in the direction of the tool velocity vector as the advancing side (AS), and the material placed in the direction opposite to the tool velocity vector as the retreating side (RS). The tool consists of two distinct parts, namely, shoulder and the unique profiled pin. The frictional heat developed due to tool rotation causes severe plastic deformation of base materials. The tool pin extrudes the softened material, and the shoulder forges it and travels along the joint line to complete the joining process [8–11]. Process parameters tool rotational speed, traverse speed, pin profile, tool tilt angle, alloy placement, and axial pressure have significant influence on weld joint quality and mechanical properties. As the FSW is a solid state process, defects present in fusion-based welding processes are eliminated. Fusion welding processes results three zones such as weld zone (WZ), heat affected zone (HAZ), and base material (BM). However, FSW consists of another additional zone, namely, thermomechanical heat affected (TMAZ) between the weld zone called as the weld nugget (NZ) or stir zone (SZ) and HAZ.

2. Literature Review

AA2024-T3 and AA7075-T6 dissimilar aluminum alloys joined by the TIG welding technique using double tungsten electrodes. They concluded that the usage of double electrodes resulted in a stable arc with an excellent weld bead appearance. However, the weld zone microhardness is lower compared to HAZ on the AA7075 alloy side. Maximum weld joint tensile strength is 44% and 37% lower than the strength of AA7075-T6 and AA2024-T3 base alloys, respectively [12]. Similar findings are observed by Sayer et al., who investigated tig and friction stir welded dissimilar AA5083 and AA2014 aluminum alloys. The obtained weld joints are characterized for tensile and hardness distribution. Weld joint tensile strength is lower than the two base alloys considered. Microhardness at the weld zone decreases sharply, which may be attributed to silicon domination in the weld zone [13]. AA5083 and AA6061 dissimilar aluminum alloys joined by the automated pulse tig welding technique with the aim to study the mechanical properties of weld joints. Nonuniform grain size and porosities presence in the weld zone resulted in hardness variation across the weld zone and a strength of the joint lower than the base alloys [14]. Similarly, Waleed and Subbaiah tig welded AA5083-H111 and AA6061-T6 aluminum alloys using ER4047 (silicon rich) filler wire. Due to usage of silicon rich filler, magnesium-silicon precipitates along the AA6061 side of the weld joint. The presence of microcavities and pores in the weld zone leads to minimum weld joint tensile strength and microhardness values [15]. TIG and FSW technique adopted to join the AA7075-T651 and AA6061-Tl dissimilar aluminum alloys. Microstructural examination reveals the presence of microvoids in the weld zone. The maximum weld zone hardness is lower than the considered alloys in both the techniques [16]. AA5083 and AA7075 aluminum dissimilar alloys successfully joined by AC-TIG welding using five different currents (80 amp to 120 amp). Weld joints fabricated at 100 amp current resulted in maximum tensile strength and elongation percentage compared to welds made at other weld currents [17]. Dissimilar AA5383 and AA7075 aluminum alloys successfully joined using friction stir welding (FSW). A tool rotational speed of 700 rpm and traverse speed 40 mm/min resulted in weld joint tensile strength of 211 MPa [18]. Dissimilar AA5754-H111 and AA7075-T651 aluminum alloys were joined with the FSW process. Defect free joint with maximum tensile strength of 239 MPa is achieved when tool traverse and rotational speeds are 80 mm/min and 1000 rpm, respectively [19]. Placing a softer alloy on the advancing side resulted in maximum weld joint tensile strength in the FSW of dissimilar AA5052-H34 and AA7075 aluminum alloys [20]. AA5083-H111 and AA7075-T651 aluminum alloys successfully joined the FSW process. The defect free joint with the maximum tensile strength (371 MPa) obtained for the weld configuration of AS5083-H111 and RS 7075-T651. Weld joint strength decreases with an increase in TRS [21]. Similar observations were found in the FSW of dissimilar AA5083-H111 and AA7075-T651 aluminum alloys [22]. In another study on FSW of AA5083-H111 and AA7075-T651 aluminum alloys, tool traverse speed significantly influenced the joint formation and grain size. High heat generation at lower traverse speed resulted in tunnel defects, whereas higher traverse speeds enhance the joint tensile strength and decreased the stir zone grain size [23].

The literature review shows that weld process parameters significantly influenced the joint formation and tensile strength. Very limited works on AA5083-O and AA7075-T651 dissimilar aluminum alloys presented in open literature. In the present study, an attempt has been made to study the effect of weld process parameters on joint formation and

mechanical properties of TIG and FSW of dissimilar AA5083-O and AA7075-T651 aluminum alloys.

3. Materials and Methods

Two aluminum alloys used in this research AA5083-O and AA7075-T651 were procured from Perfect Metal works, Bangalore, India. The chemical composition of the plates were tested by using a spectroscope and detailed report is presented in Table 1.

Rolled sheets of two considered base alloys AA5083-O and AA7075-T651 are cut into $100 * 75 * 3$ size using water jet cutting process. TIG welding is performed at five different weld currents (80 amp–120 amp) using EWM 500 Tetrix 500 AC/DC machine. Friction stir welding (FSW) of base alloys carried on an NC FSW machine (Make: R.V. Machine tools, Coimbatore). Tool rotational speeds 800 rpm, 1000 rpm, 1100 rpm, 1200 rpm, and 1400 rpm with a constant traverse speed 40 mm/min employed for fabrication of weld joints. A straight square probe profile is used for weld joint fabrication. Samples were cut perpendicular to the joint lines of both fabricated plates for metallographic examination. All the samples were prepared as per the standard metallographic procedure and etched with Keller solution for AA7075-T651 and Poulton solution for AA5083-O. All the fabricated joints were characterized for microhardness measurement across the joint line with 1 mm spacing between indentations, 15 s duration, and 500 g indentation force. According to ASTM E8 samples were prepared for tensile testing. Tensile characteristics of all the weld joints were performed on a computerized universal testing machine (Made: INSTRON 8801) with a strain rate of 10^{-1} S^{-1}.

4. Results and Discussion

4.1. Microstructural Analysis. Tensile characterization of all the fabricated joints reveals that joints fabricated at 100 amp weld current in TIG and at 1100 rpm tool rotational speed in FSW exhibited superior joint strength to those welds made at other process parameters. Hence, metallurgical and mechanical characterization conducted for the weld joints showed superior tensile strength. Microstructural examination in the vertical section of weld fabricated at 100 amp current shown in Figures 1 and 2 in a particular direction grain elongation takes place and highly equiaxed grains in the weld center are observed. At the weld top grains are highly elongated, whereas at the bottom, abnormal grain growth resulted due to generation of severe heat during the TIG welding process [17].

Similarly, the macrostructure and stir zone (SZ) microstructure of the weld joint fabricated at 1100 rpm tool rotational speed presented in Figures 3 and 4, respectively. In FSW heat generation directly affects the dissolution of strengthening precipitates and the dynamic recrystallization of base material grains [7–9]. Tool rotational and traverse speed decides the amount of heat generated during the process [20, 24]. Heat generation is minimum at low rotational speed; further fine grains are expected in SZ. Higher tool rotational speeds result in severe heat generation and coarse grains expected. Insufficient and severe heat generation, respectively, at low and high rotational speeds resulted in fine and coarse grains [20, 21, 25, 26]. Microstructural images of the both weld joints shown a variety of grain orientation and size. The fusion zone microstructure of the TIG weld completely differs with SZ microstructure of the FSW joint. This difference could be attributed to the variation in heat input and dynamic recrystalization in the FSW process. Low grain size and an increase in grain boundaries could be the reason for superior join strength in FSW joints compared to the TIG samples.

4.2. Scanning Electron Microscopy Study (SEM). Weld joints fabricated at 100 amp current in TIG and 1100 rpm rotational speed in FSW are characterized for SEM analysis. SEM micrograph presented in Figure 5 supports the microstructural analysis presented in Figure 2 for the weld joint fabricated by fusion welding technique. Dispersoid dissolution in the fusion zone is responsible for superior strength of weld joint produced at 100 amp current. Figure 5 illustrates microconstituents and nodules presence during the solidification weld metal. Secondary segregated microconstituents during weld metal solidification could be due to the magnesium dilution at later stages of the welding process [17]. Thus, it further helps in reducing solidification cracking which confirmed by the absence of a crack at center of the weldment fabricated at 100 amp.

Similarly, Figure 6 depicts the SEM micrograph of the weld joint fabricated at 1100 rpm tool rotational speed. In FSW heat generation is responsible for the strength of the weld joint and proper bonding between the base materials. Friction between the base material and the tool shoulder affects heat generation. Which are further significantly affected by the process parameters such as rotational speed, traverse speed, pin profile, and base materials. However, among the mentioned parameters, tool rotational speed stood first as having influence on heat generation. At lower rotational speed generated heat is not sufficient to solidify the base materials and joint formation [7–9]. On the other hand, at higher tool rotational speeds, excessive heat generation causes overflow of solidified materials and defect formation. Figure 4 shows the formation dispersion and reprecipitates in SZ of the weld joint produced at 1100 rpm. Dissolution of strengthening precipitates in the weld zone could be the reason behind higher joint tensile strength [10, 11].

4.3. MicroHardness. All the weld joints are characterized for microhardness measurement along the joint line and presented in Figure 7. In TIG-welded joints joint-line hardness increases with the weld current. Weld joints made at minimum weld current (80 amp) resulted in a hardness of 115 Hv, whereas, the highest joint line hardness of 138 Hv was obtained for the welds fabricated at 120 amp. It could be

Table 1: Chemical composition of base alloys and electrode used in TIG.

Base alloys and electrodes	Element (in wt. %)								
	Si	Fe	Cu	Mn	Mg	Cr	Zn	Ti	Aluminum
AA7075-T651	0.04	0.15	1.3	0.02	2.3	0.19	5.4	0.05	Balance
AA5083-O	0.09	0.27	0.01	0.8	4.4	0.07	0.02	0.02	Balance
ER5083	0.09	0.27	0.01	0.8	4.4	0.07	0.02	0.02	Balance

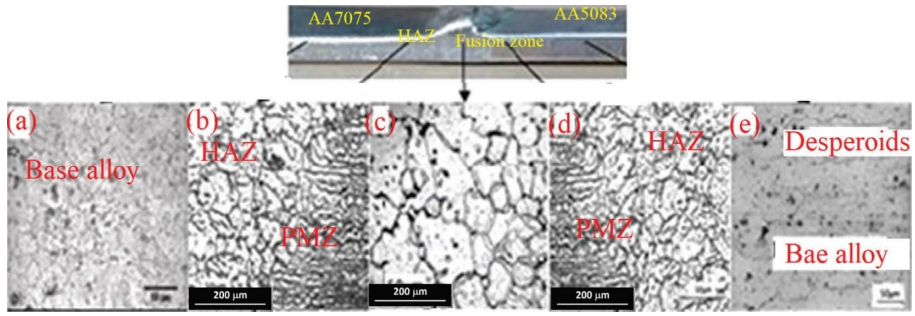

Figure 1: Macrosection of weld joint fabricated at 100 amp.

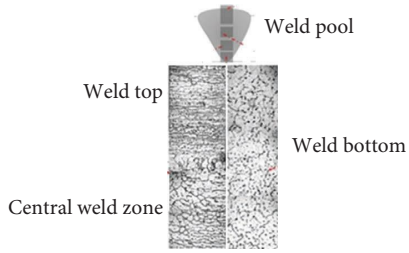

Figure 2: Microstructure of weld fabricated at 100 amp.

Figure 3: Macrostructures of the weld joint fabricated at 1100 rpm.

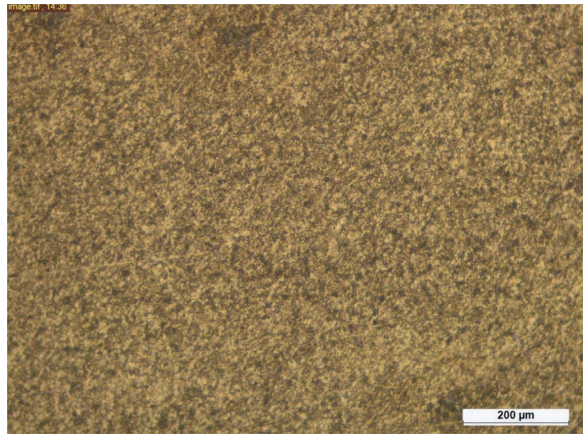

Figure 4: Stir zone microstructure of a weld joint fabricated at 1100 rpm.

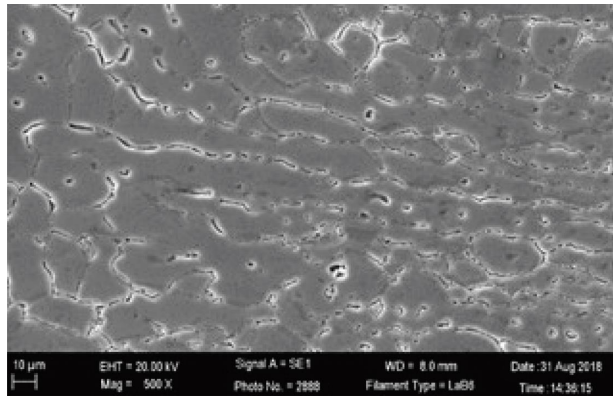

Figure 5: SEM micrograph of the weldment fabricated at 100 amp.

attributed to heat generation during the process resulting in over aging and dissolution of strengthening precipitates [17]. Joint line hardness of FSW samples exhibited lesser values compared to the TIG weld joints. The joint line hardness obtained in all FSW samples is nearly 80 Hv which is almost the same as the base alloy (AA5083-O) hardness. In the FSW tool rotational motion moves the plasticized material from leading to trailing edge. As in the present study the weld configuration is AS 5083 and RS 7075-T651, it confirms that in SZ, the alloy on the advancing side is more dominant [9, 11]. Alloy placement during the FSW process highly affects the hardness distribution and stir zone hardness values [22–26]. In works on similar alloys, the average stir zone hardness is 165 Hv which is almost near to base alloy (AA7075-T651) for the weld configuration AS7075-T651 and RS 5083-O [21]. This could be the reason that the obtained joint line hardness values in FSW samples are lower than the TIG weld joints.

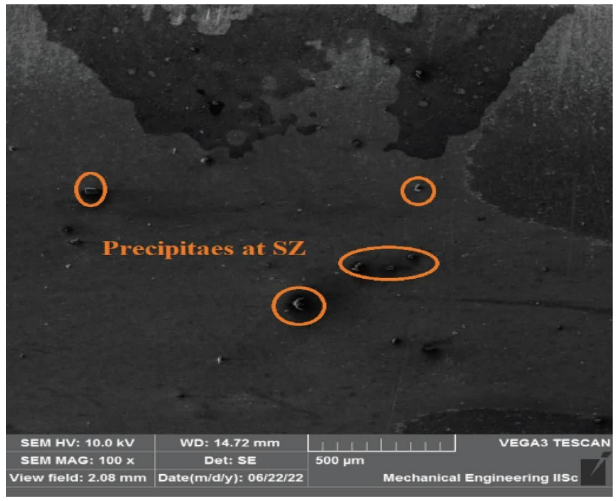

Figure 6: SEM micrograph of the weldment fabricated at 1100 rpm.

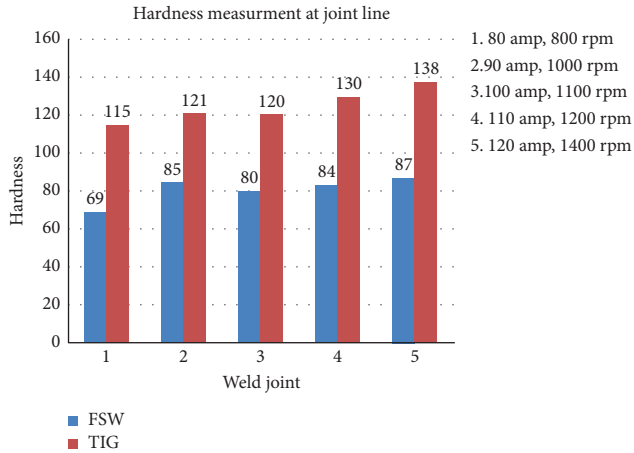

Figure 7: Microhardness at joint line of weldments.

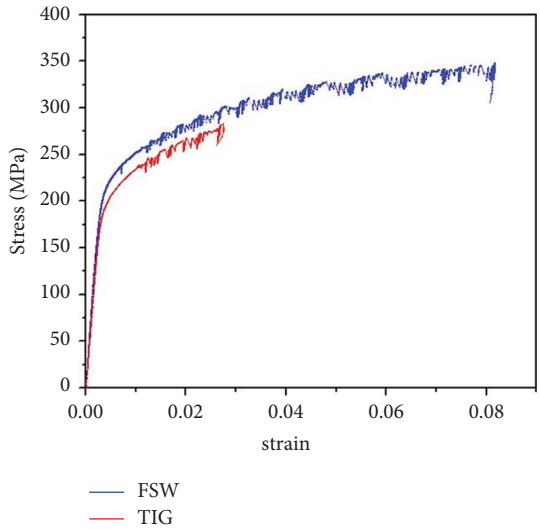

Figure 8: Stress and strain graph for TIG and FSW weld joints.

Table 2: Tensile strength of fabricated weld joints.

FSW tool rotational speed (rpm)	Tensile strength (FSW) in MPa	TIG weld current (amp)	Tensile strength (TIG) in MPa
800	208	80	205
1000	301	90	278
1100	345	100	283
1200	334	110	269
1400	215	120	239

4.4. Tensile Strength. The tensile characterization of the samples fabricated at 100 amp in TIG and 1100 rpm in FSW, as shown in Figure 8 and tensile strength of all the fabricated joints presents in Table 2. Joint tensile strength of 345 MPa and 283 MPa, respectively, obtained for TIG and FSW weld joints. It shows that the strength of FSW joints reaches base alloy (AA5083-O) strength, whereas, the strength of TIG weld joint is lower than the base alloys. In TIG welding temperature during the process is much higher than the recrystallization temperature of the base alloys [17]. Dissolution and strengthening precipitate overaging due to temperature, leads to a decrease in the strength of the joint. In FSW, joining takes place at the solid state because the temperature developed is lower than the melting temperature of base alloys and dynamic recrystallization during the process results in better joint strength. At the lower tool rotational speed, the heat generated is not sufficient to form a sound joint and the higher tool rotational speed generates more heat which further causes a decrease in tensile strength of the weld joint [20–23]. Differences in the strain hardening nature of the base alloys causes fluctuation in the tensile graph. In addition, microdefects like pores and kissing bonds could affect the tensile strength fluctuations.

5. Conclusions

The present study shows that dissimilar AA5083-O and AA7075-T651 aluminum alloys can successfully be joined by TIG and FSW techniques. The following conclusions can be drawn from this investigation.

Weld joints fabricated at 100 amp current in TIG welding resulted in a tensile strength of 283 MPa. Heat input significantly affected the defect formation and tensile joint strength of weld joints. Over aging and grain coarsening affected the joint line hardness. Joints made by the FSW process showed the highest tensile strength of 341 MPa. Defect-free joints can be achieved through FSW with selection of proper process parameters. Joints fabricated at low and high tool rotational speeds resulted with an insufficient and severe heat input, respectively. Insufficient heat input resulted in low tool rotational speeds affected the joint tensile strength. Dissolution and over aging of strengthening precipitates caused minimum strength in TIG welded samples, and dynamic recrystallization resulted in fine and equiaxed grains for the weld joints made with FSW, which showed superior strength.

Data Availability

The data used to support the findings of this study are included within the article.

Conflicts of Interest

The authors declare that there are no conflicts of interest.

References

[1] R. Raja, A. Parthiban, S. Nandha Gopan, and D. Degefa, "Investigate the process parameter on the friction stir welding of dissimilar aluminium alloys," *Advances in Materials Science and Engineering*, vol. 2022, p. 8, 2022.

[2] G. G. Krishna, "Improving joint strength of the friction stir welding of dissimilar aluminium alloy by using coating technique," *Sådhanå*, vol. 47, p. 7, 2022.

[3] M. Nagaaravindaraj, J. Ragavan, B. Muthuselvam, and K. Chandarasekaran, "Influence of process parameters on AA7075 inTIG welding," *International Journal of Advanced Research in Technology, Engineering and Science*, vol. 2, no. 2, pp. 13–18, 2015.

[4] R. Padmanaban, V. Balusamy, and R. Vaira Vignesh, "Effect of friction stir welding process parameters on the tensile strength of dissimilar aluminum alloy AA2024-T3 and AA7075-T6 joints," *Materialwissenschaft und Werkstofftechnik*, vol. 51, no. 1, pp. 17–27, 2020.

[5] R. Rudrapati, "Effects of welding process conditions on friction stir welding of polymercomposites: a review," *Composites Part C: Open Access*, vol. 8, Article ID 100269, 2022.

[6] A. Kumar and S. Sundarrajan, "Optimization of pulsed TIG welding process parameters on mechanical properties of AA 5456 Aluminum alloy weldments," *Materials & Design*, vol. 30, no. 4, pp. 1288–1297, 2009.

[7] Z. Y. Ma, A. H. Feng, D. L. Chen, and J. Shen, "Recent advances in friction stir welding/processing of aluminum alloys: microstructural evolution and mechanical properties," *Critical Reviews in Solid State and Materials Sciences*, vol. 43, no. 4, pp. 269–333, 2017.

[8] R. Palanivel, P. Koshy Mathews, N. Murugan, and I. Dinaharan, "Effect of tool rotational speed and pin profile on microstructure and tensile strength of dissimilar friction stir welded AA5083-H111 and AA6351-T6 aluminum alloys," *Materials & Design*, vol. 40, pp. 7–16, 2012.

[9] C. Hamilton and M. Kopyscianski, "Aleksandra We˛glowska, Adam Pietras and Stanisław Dymek, Modeling, microstructure, and mechanical properties of dissimilar 2017A and 5083 aluminum alloys friction stir welds," *Journal of Engineering Manufacture*, vol. 233, no. 2, pp. 1–12, 2017.

[10] P. L. Threadgill, A. J. Leonard, H. R. Shercliff, and P. J. Withers, "Friction stir welding of aluminium alloys," *International Materials Reviews*, vol. 54, no. 2, pp. 49–93, 2009.

[11] M. Ilangovan, S. Rajendra Boopathy, and V. Balasubramanian, "Effect of tool pin profile on microstructure and tensile properties of friction stir welded dissimilar AA 6061–AA 5086 aluminium alloy joints," *Defence Technology*, vol. 11, no. 2, pp. 174–184, 2015.

[12] L. Kaba, M. E. Djeghlal, S. Ouallam, and S. Kahla, "Dissimilar welding of aluminum alloys 2024 T3 and 7075 T6 by TIG process with double tungsten electrodes," *The International Journal of Advanced Manufacturing Technology*, vol. 118, no. 3-4, pp. 937–948, 2022.

[13] S. Sayer, C. Yeni, and O. Ertugrul, "Comparison of mechanical and microstructural behaviors of tungsten inert gas welded and friction stir welded dissimilar aluminum alloys AA 2014 and AA 5083," *Metallic Materials*, vol. 49, no. 2, pp. 155–162, 2011.

[14] P. K. Baghel and D. S. Nagesh, "Mechanical properties and microstructural characterization of automated pulse TIG welding of dissimilar aluminum alloy," *Indian Journal of Engineering and Materials Sciences*, vol. 25, pp. 147–154, 2018.

[15] W. A. Waleed and K. Subbaiah, "E ect of ER4047 filler rod on tungsten inert gas welding of AA5083-H111 and AA6061-T6 aluminum alloys," *Journal of Chemical and Pharmaceutical Sciences*, vol. 7, pp. 210–213, 2017.

[16] C. Patil, H. Patil, and H. Patil, "Experimental investigation of hardness of FSW and TIG joints of Aluminium alloys of AA7075 and AA6061," *Frattura Ed Integrità Strutturale*, vol. 10, no. 37, pp. 325–332, 2016.

[17] G. Veeraiah, N. Ramanaiah, I. Sudhakar, and K. Venkateswarlu, *Influence of AC-TIG weld Current on Dissimilar AA5083 and AA 7075 Aluminium alloy*, 2022.

[18] S. Sivachidambaram, G. Rajamurugan, and D. Amirtharaj, "Optimizing the parameters for friction stir welding of dissimilar aluminium alloys AA5383/AA7075," *ARPN Journal of Engineering and Applied Sciences*, vol. 10, pp. 5434–5437, 2015.

[19] S. Kasman and Z. Yenier, "Analyzing dissimilar friction stir welding of AA5754/AA7075," *The International Journal of Advanced Manufacturing Technology*, vol. 70, no. 1-4, pp. 145–156, 2014.

[20] A. Z. Ahmed, M. K. Abbass, A. H. Ataiwi, S. K. Khanna, B. Jashti, and C. Widener, "Investigation of fatigue behavior and fractography of dissimilar friction stir welded joints of aluminum alloys 7075-T6 and 5052-H34," *International Journal of Materials Science and Engineering*, vol. 2, pp. 115–121, 2014.

[21] I. Kalemba-Rec, M. Kopyściański, D. Miara, and K. Krasnowski, "Effect of process parameters on mechanical properties of friction stir welded dissimilar 7075-T651 and 5083-H111 aluminum alloys," *The International Journal of Advanced Manufacturing Technology*, vol. 97, no. 5-8, pp. 2767–2779, 2018.

[22] I. Kalemba-Rec, C. Hamilton, M. Kopyściański, D. Miara, and K. Krasnowski, "Microstructure and mechanical properties of friction stir welded 5083 and 7075 aluminum alloys," *Journal of Materials Engineering and Performance*, vol. 26, no. 3, pp. 1032–1043, 2017.

[23] M. Saeidi, B. Manafi, M. Besharati Givi, and G. Faraji, "Mathematical modeling and optimization of friction stir welding process parameters in AA5083 and AA7075 aluminum alloy joints," *Proceedings of the Institution of Mechanical Engineers - Part B: Journal of Engineering Manufacture*, vol. 230, no. 7, pp. 1284–1294, 2016.

[24] M. Ramamurthy, P. Balasubramanian, N. Senthilkumar, and G. Anbuchezhiyan, "Influence of process parameters on the microstructure and mechanical properties of friction stir welds of AA2014 and AA6063 aluminium alloys using response surface methodology," *Materials Research Express*, vol. 9, no. 2, p. 026528, 2022.

[25] R. Madhusudhan, M. M. M. Sarcar, N. Ramanaiah, and K. PrasadaRao, "An experimental study on the effect of weld parameters on mechanical and micro structural properties of dissimilar aluminium alloy FS welds," *International Journal of Modern Engineering Research (IJMER)*, vol. 2, no. 4, pp. 1459–1463.

[26] R. Raja, A. Parthiban, S. Jeyakumar, and B. Radha Krishnan, "Investigation of mechanical properties of friction stir welding aluminium alloy AA7475-T651 and AA2219-O," *Materials Today: Proceedings*, vol. 60, pp. 1421–1423, 2022.